

# **Doctoral Dissertation**

## **Tracking atmospheric chemical components in accordance with the Sustainable Development Goals (SDGs)**

Phan Anh

November 15, 2023

Graduate School of Engineering  
Chubu University

A Doctoral Dissertation  
submitted to Graduate School of Engineering,  
Chubu University  
in partial fulfillment of the requirements for the degree of  
Doctor of ENGINEERING

Phan Anh

Thesis Committee:

Professor Hiromichi Fukui (Supervisor)  
Professor Kiyoshi Honda (Chubu University)  
Professor Jun Izutsu (Chubu University)  
Professor Masao Takano (Nagoya University)

# **Tracking atmospheric chemical components in accordance with the Sustainable Development Goals (SDGs)\***

Phan Anh

## **Abstract**

Lorem ipsum dolor sit amet, consectetur adipisicing elit, sed do eiusmod tempor incididunt ut labore et dolore magna aliqua. Ut enim ad minim veniam, quis nostrud exercitation ullamco laboris nisi ut aliquip ex ea commodo consequat. Duis aute irure dolor in reprehenderit in voluptate velit esse cillum dolore eu fugiat nulla pariatur. Excepteur sint occaecat cupidatat non proident, sunt in culpa qui officia deserunt mollit anim id est laborum.

Lorem ipsum dolor sit amet, consectetur adipisicing elit, sed do eiusmod tempor incididunt ut labore et dolore magna aliqua. Ut enim ad minim veniam, quis nostrud exercitation ullamco laboris nisi ut aliquip ex ea commodo consequat. Duis aute irure dolor in reprehenderit in voluptate velit esse cillum dolore eu fugiat nulla pariatur. Excepteur sint occaecat cupidatat non proident, sunt in culpa qui officia deserunt mollit anim id est laborum.

## **Keywords:**

$\pi$ , astronomy, mathematics, computer, algorithm

---

\*Doctoral Dissertation, Graduate School of Information Science,  
Nara Institute of Science and Technology, November 15, 2023.

# Contents

<b>List of Figures</b>	<b>iv</b>
<b>List of Tables</b>	<b>1</b>
<b>1 Introduction</b>	<b>2</b>
1.1 Background . . . . .	2
<b>2 Background</b>	<b>3</b>
2.1 Air pollution . . . . .	3
2.2 Greenhouse gas . . . . .	3
<b>AIR POLLUTION INDUCED BY INTERVENTION EVENTS</b>	<b>4</b>
<b>3 Ukraine's case study</b>	<b>5</b>
3.1 Introduction . . . . .	5
3.2 Data . . . . .	8
3.2.1 Selection of analysis periods . . . . .	8
3.2.2 TROPOMI NO <sub>2</sub> from Sentinel 5P . . . . .	9
3.2.3 Meteorological and surface NO <sub>2</sub> data . . . . .	12
3.2.4 Fire spots database and Ukraine crisis hub . . . . .	13
3.2.5 Population data . . . . .	14
3.3 Business-as-usual (BAU) modelling . . . . .	14
3.4 NO <sub>2</sub> changes induced by COVID-19 lockdown . . . . .	16
3.4.1 Lockdown and pre-lockdown meteorological patterns . . . . .	17
3.4.2 S5P NO <sub>2</sub> level changes in the most populous cities of Ukraine	17
3.5 NO <sub>2</sub> changes induced by the armed conflict . . . . .	21
3.5.1 Changes of S5P NO <sub>2</sub> levels in conflict hotspot locations . . . . .	22
3.5.2 Changes of S5P NO <sub>2</sub> levels in other affected areas . . . . .	26

3.6 Conclusion . . . . .	28
<b>4 Japan's case study</b>	<b>33</b>
<b>GREENHOUSE GAS ESTIMATION AND MONITORING</b>	<b>34</b>
<b>5 Plant functional types mapping based on scared data</b>	<b>35</b>
<b>6 Global upscaled of carbon fluxes</b>	<b>36</b>
<b>7 CO<sub>2</sub> monitoring and net zero modelling platform</b>	<b>37</b>
<b>8 Conclusion</b>	<b>38</b>
<b>Bibliography</b>	<b>40</b>

# List of Figures

3.1	Monthly (February to July) average map of TROPOMI S5P NO <sub>2</sub> tropospheric columns for Ukraine from 2019 to 2022 using ORG data . . . . .	10
3.2	Monthly (February to July) average map of TROPOMI S5P NO <sub>2</sub> tropospheric columns for Ukraine from 2019 to 2022 using RPRO data . . . . .	10
3.3	Monthly (from February to July) number of TROPOMI S5P NO <sub>2</sub> tropospheric columns observations for Ukraine from 2019 to 2022 using ORG data . . . . .	11
3.4	Monthly (from February to July) number of TROPOMI S5P NO <sub>2</sub> tropospheric columns observations for Ukraine from 2019 to 2022 using RPRO data . . . . .	11
3.5	Probability density functions of BLH during (a) the pre-lockdown (March 1–15) and (b) the lockdown period (April 6–May 10) between 2019 and 2020 based on data from the nine most populous cities of Ukraine. Wind rose plots for wind speed and direction for pre-lockdown (March 1–15) and lockdown (April 6–May 10) periods in (c) 2019 and (d) 2020 based on data from the nine most populous cities of Ukraine . . . . .	18
3.6	Estimates of S5P NO <sub>2</sub> column changes for the nine most populous cities in Ukraine during the (a) pre-lockdown and (b) lockdown periods. . . . .	20
3.7	Satellite-captured fire spots for 2021 (1st column), 2022 (2nd column) and conflict hotspots (3rd column) in April, May, June and July. The patterns of conflict hotspots are clearly recognizable in the satellite-capture fire product from NASA FIRMS . . . . .	23

3.8 OBS-BAU and year-to-year estimates for the individual conflict events including air/drone strikes, armed clashes, remote explosive/landmine occurrences, shelling/artillery/missile attacks, and other forms of attacks that occurred between February 24 and July 31, 2022, for five frontline oblasts, Dnipropetrovsk, Donetsk, Kharkiv, Luhansk and Zaporizhzhia. The number of data points is denoted by (n). . . . .	25
3.9 The trend lines of OBS and BAU S5P NO <sub>2</sub> column levels from February to July in 2020 and 2022 for five cities in Ukraine. Each row displays plots for a different city. The first and second column plots represent the ORG data (S5P version 1.x), while the third and last column plots show the RPRO data (S5P version 2.4). The first and third column plots pertain to 2020, while the second and last column plots pertain to 2022. . . . .	27
3.10 The trend lines for the OBS and BAU S5P NO <sub>2</sub> column levels from February to July in 2020 and 2022 are presented for selected CPPs. Each row displays plots for a different CPP. The first and second column plots represent ORG data (S5P version 1.x), while the third and last column plots show RPRO data (S5P version 2.4). The first and third column plots pertain to 2020, while the second and last column plots pertain to 2022. . . . .	29

## List of Tables

# 1 Introduction

## 1.1 Background

## **2 Background**

### **2.1 Air pollution**

### **2.2 Greenhouse gas**

  Lorem ipsum dolor sit amet, consectetur adipisicing elit, sed do eiusmod tempor incididunt ut labore et dolore magna aliqua. Ut enim ad minim veniam, quis nostrud exercitation ullamco laboris nisi ut aliquip ex ea commodo consequat. Duis aute irure dolor in reprehenderit in voluptate velit esse cillum dolore eu fugiat nulla pariatur. Excepteur sint occaecat cupidatat non proident, sunt in culpa qui officia deserunt mollit anim id est laborum.

# **AIR POLLUTION INDUCED BY INTERVENTION EVENTS**

# 3 Ukraine's case study

## 3.1 Introduction

Nitrogen dioxide ( $\text{NO}_2$ ) is a key air pollutant that can have harmful effects on human health. An increase in nitrogen oxide ( $\text{NOx} = \text{NO} + \text{NO}_2$ ) concentrations contributes to global warming through a chemical reaction that leads to the formation of ozone ( $\text{O}_3$ ), a short-lived climate pollutant with a potent warming effect (Stocker et al., 2013). The lifetime of  $\text{NO}_2$  is strongly influenced by photochemical reactions and meteorological parameters (Barré et al., 2021) and varies seasonally (Dragomir et al., 2015; Kendrick et al., 2015). During winter, photochemical reaction activity is reduced, resulting in a longer lifetime of the  $\text{NO}_2$ . Additionally, seasonal variations in  $\text{NO}_2$  concentration are controlled by dispersion processes which are significantly affected by changes in boundary layer height (BLH), wind speed and direction patterns due to temperature inversions in summer and winter (Barré et al., 2021; Kendrick et al., 2015).  $\text{NO}_2$  concentration levels have been widely used to evaluate decreases in emissions associated with intervention events such as the COVID-19 pandemic lockdown and impacts on the air quality due to the short lifetime of  $\text{NO}_2$  in the atmosphere (Barré et al., 2021; Cooper et al., 2022). In Europe, anthropogenic  $\text{NOx}$  emissions are mainly attributed to combustion processes in transportation, as well as energy production and distribution.

In Ukraine, coal-fired power plants (CPPs) dominantly account for 80% of total  $\text{SO}_2$  and 25% of total  $\text{NOx}$  emissions, and some have been identified as the highest-emitting CPPs in the region and in the world (Lauri and Rosa, 2021). Since the pandemic started in March 2020, and now with the ongoing armed conflict with Russia, Ukraine has faced a series of threats to the economy, human security and the environment, as well as geopolitical tensions (Pereira et al.,

2022). During the pandemic response starting in 2020, many national and local lockdown restrictions were issued to prevent the spread of the virus, causing a sharp decrease in gross domestic product growth rate, as well as industrial and energy production (Danylyshyn, 2020). In 2021, Ukraine's economy started to recover from the pandemic but the recovery was eventually upended by an armed conflict with Russia that started on February 24, 2022. The conflict has been causing a multi-pronged crisis not only in Ukraine but also in Europe, with increased prices and exacerbated inflation among the many impacts. Many facilities and extensive areas of housing and other infrastructure, including some CPPs, have been reported destroyed or damaged in Ukraine. These impacts have consequently triggered an unprecedented refugee crisis in Ukraine, clogging border crossings between Ukraine and bordering European countries (Júlia et al., 2022). The many socio-economic changes that have occurred during the pandemic and the conflict could be expected to contribute to major variability in air quality in Ukraine, including NO<sub>2</sub> pollution levels, during the 2020–2022 period.

A report by the United Nations Development Programme (UNDP) (Dumitru et al., 2020), estimated the impacts of the pandemic lockdown on NO<sub>2</sub> levels in Ukraine by using Sentinel 5P (S5P) NO<sub>2</sub> column concentrations and Copernicus Atmosphere Monitoring Service (CAMS) surface NO<sub>2</sub> data (Marécal et al., 2015). However, meteorological variables were not acknowledged, although ignoring weather factors could strongly affect final estimates of changes in pollution concentration levels induced by the lockdown (Schiermeier, 2020). A more recent study (Zalakeviciute et al., 2022) utilized direct satellite observation from 2019 and early 2020 as business-as-usual data to evaluate the impact of the Russia-Ukraine conflict in 2022 on air quality, but again, without acknowledging weather effects. These two studies utilized estimates of year-to-year differences. However, such estimates can easily be affected and dominated by changes in meteorological parameters rather than emission sources (Grange et al., 2021; Shi et al., 2021). Therefore, a more sophisticated method is needed to measure the impacts of intervention events through better quantification of actual air quality.

In order to normalize the meteorological effects to accurately and reliably quantify the impact of intervention events, the use of machine learning is increasingly being adopted, but mostly applied for ground-based measurements following the

original idea proposed by (Grange et al., 2018) and (Grange and Carslaw, 2019). The objective of this approach is to construct a business-as-usual (BAU) model for predicting air pollution levels independently of the impacts of any intervention events. This is achieved by integrating meteorological, spatial, and temporal features into the model during the BAU period to accurately represent air pollution levels. An intervention event, in this context, refers to an occurrence that has caused changes in air quality. Recently, (Barré et al., 2021) have introduced their weather normalization approach to improve estimates of lockdown impacts not only on NO<sub>2</sub> levels from ground-based observations and CAMS simulations, but also in satellite measurements from S5P. The original method in (Grange et al., 2018; Grange and Carslaw, 2019) has been altered in order to work with satellite retrieval column NO<sub>2</sub> concentration levels from S5P by adopting a new feature, the forecast surface NO<sub>2</sub> level from CAMS data. Alternatively, gradient boosting machines (GBMs) (Friedman, 2001) have been also utilized instead of random forests (Grange et al., 2018) to develop weather-normalization models under the BAU conditions. (Barré et al., 2021) reported an overall reduction (ranging from 23% to 32%) in major European cities using the three datasets. Their study showed an average difference of 14% between satellite-based and ground-based estimates, and 11% between simulations from the CAMS regional ensemble of air quality models and ground-based estimates. These findings suggest that estimates of the impacts of the lockdown on NO<sub>2</sub> levels can vary depending on the source of the data.

This chapter aims to investigate the actual satellite-derived column NO<sub>2</sub> pollution levels induced by pandemic lockdown restrictions and the armed conflict with Russia, which have been two major changes in human activities in Ukraine since 2019. In order to do so, we developed a weather-normalization model under BAU scenarios for S5P column NO<sub>2</sub> levels to decouple the meteorological effects from the intervention effects. The BAU simulation NO<sub>2</sub> levels are then used to quantify changes in S5P column NO<sub>2</sub> concentrations during the lockdown and the armed conflict. We describe the data used in the study in section 3.2 and the methodology in section 3.3. The results and discussion on NO<sub>2</sub> level changes are summarized in section 3.4 for the lockdown, and section 3.5 for the armed conflict. Finally, we conclude the results of the study in section 3.6.

## 3.2 Data

### 3.2.1 Selection of analysis periods

In this study, we consider the three years 2019, 2020, and 2022 for our analysis. We assumed that in 2019, before the lockdown in 2020 and the armed conflict with Russia in 2022, there were no other significant factors impacting socio-economic activities. Hence, we used 2019 NO<sub>2</sub> pollution levels as the reference data for development of the BAU model.

Ukraine reported its first active case of COVID-19 on March 3, 2020, and began closing its borders to foreign citizens from March 15 onwards. Around the same time, the country also witnessed its first COVID-19 related death. On April 6, the government introduced a strict lockdown, imposing significant restrictions on movement and requiring the public to wear masks in public spaces. This lockdown was eventually extended until June, although certain restrictions were already lifted starting from May 11. For the lockdown component of our study, we focused on two specific periods: the pre-lockdown period, which ran from March 1 to 15, 2020, and the strict lockdown period, spanning from April 6 to May 10, 2020. The decision to count the pre-lockdown period from March 1 was based on the lack of qualified S5P data available for analysis before March, as indicated in Figure 2. In 2021, even though COVID-19 vaccines had been developed and distributed to citizens of Ukraine (vaccinations started on February 24, 2021), many local lockdowns and restrictions continued to be issued to cope with growing numbers of daily COVID-19 active cases, while trying to keep socio-economic activities on track for recovery.

The Russia-Ukraine conflict began on February 24, 2022. We employed data for the period February 1 to July 31 each year from 2019 to 2022 for NO<sub>2</sub> variability analysis. This time frame covers the pre-lockdown and lockdown periods in 2020 and extends beyond the first five months (February 24 to July 31) of the armed conflict in 2022.

### 3.2.2 TROPOMI NO<sub>2</sub> from Sentinel 5P

Most previous studies assessing the impacts of intervention involved ground observations in their analysis. However, reliable ground measurement data was only available in Kyiv (capital of Ukraine) as other sites had been damaged or destroyed in the armed conflict and taken out of service (Savenets, 2021). Thus, open satellite data is considered the most efficient way to monitor air quality for all parts of Ukrainian territory (Shelestov et al., 2021).

The S5P data has been distributed from 2018 to the present with two available options. The first is original data (ORG) processed with either of two versions of processor, v1.x (5/2018–6/2021) or v2.x (7/2021 onwards). The second is reprocessed datasets (RPRO) with the processor (v2.x) for the full mission. According to (Van Geffen et al., 2022), the S5P NO<sub>2</sub> v2.2 data has larger vertical column density (VCDs) than v1.x data, ranging from 10% to 40%, mostly found at mid and high latitudes in winter. Therefore, bias between S5P v1.x and v2.x could lead to overestimation and underestimation when comparing air pollution data in 2022 versus 2019, thereby affecting evaluations of the conflict’s impacts on S5P NO<sub>2</sub> levels.

In this study, we conducted experiments using two versions of S5P NO<sub>2</sub> data. The first dataset is ORG data which was collected through level 3 (L3) offline processing (OFF) of the S5P product available on Google Earth Engine (Gorelick et al., 2017). This dataset comprises processed data from different processor versions for each year from 2019 to 2022 (v1.3.1 in 2019, v1.3.2 in 2020, and v2.3.1 in 2022). The second dataset, denoted as the RPRO product, employs processor version v2.4.0 for the full mission duration. This dataset was acquired from the Sentinel-5P Pre-Operations Data Hub ([s5phub.copernicus.eu](http://s5phub.copernicus.eu)) using the Sentinelsat API.

Regarding the RPRO data, we began by downloading the level 2 (L2) dataset. In order to generate the L3 NO<sub>2</sub> dataset, each operational L2 product underwent mosaicking and filtering of low-quality pixels, which involved removing items with quality assurance (QA) values less than 75% for the “tropospheric\_NO<sub>2</sub>\_column\_number\_density” band. The harpconvert tool was utilized to perform the conversion from L2 to L3 product. Subsequently, both datasets were linearly interpolated to a spatial resolution of 0.1×0.1 degree. At

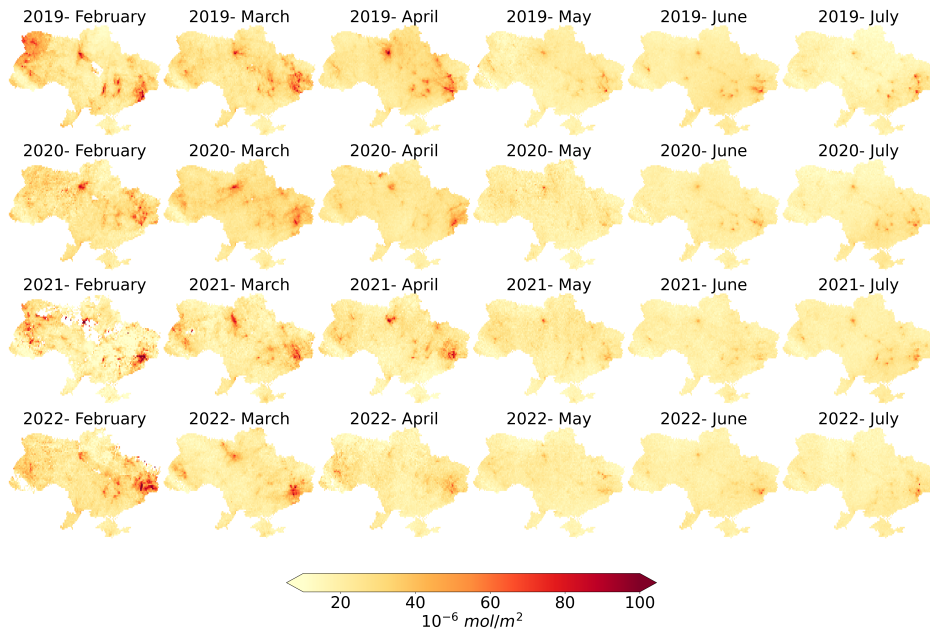


**Figure 3.1.** Monthly (February to July) average map of TROPOMI S5P NO<sub>2</sub> tropospheric columns for Ukraine from 2019 to 2022 using ORG data.

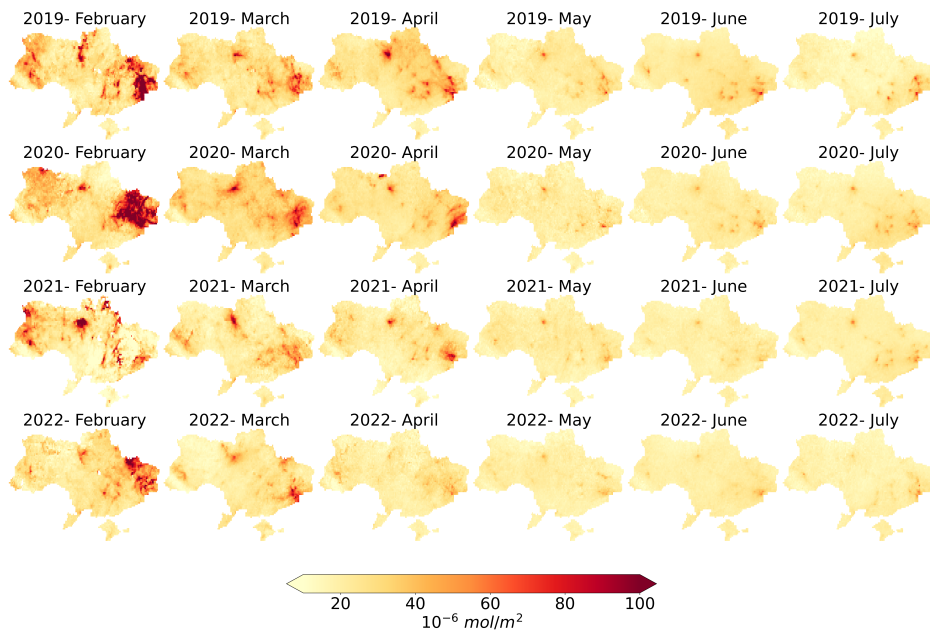


**Figure 3.2.** Monthly (February to July) average map of TROPOMI S5P NO<sub>2</sub> tropospheric columns for Ukraine from 2019 to 2022 using RPRO data

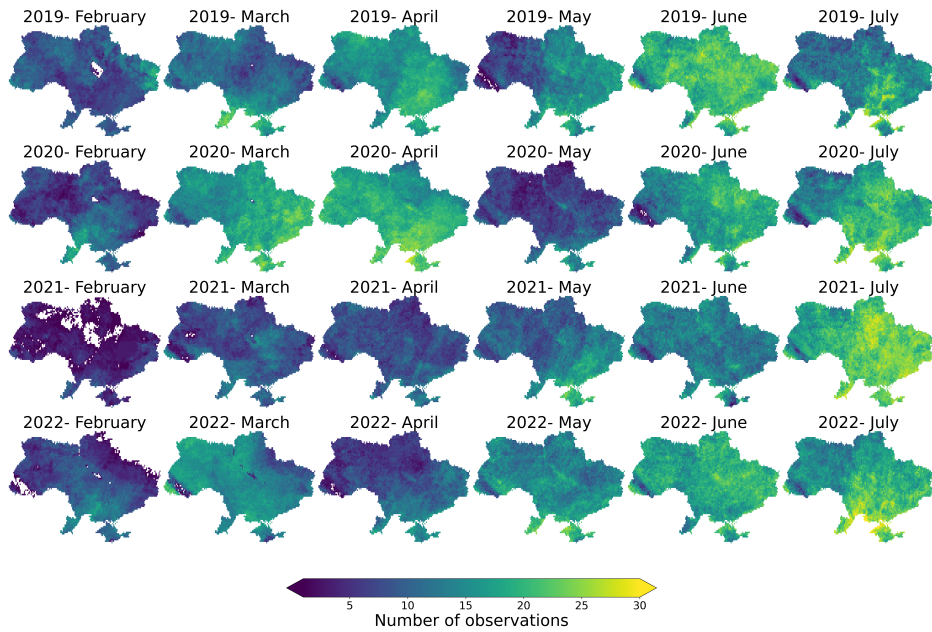


**Figure 3.3.** Monthly (from February to July) number of TROPOMI S5P NO<sub>2</sub> tropospheric columns observations for Ukraine from 2019 to 2022 using ORG data

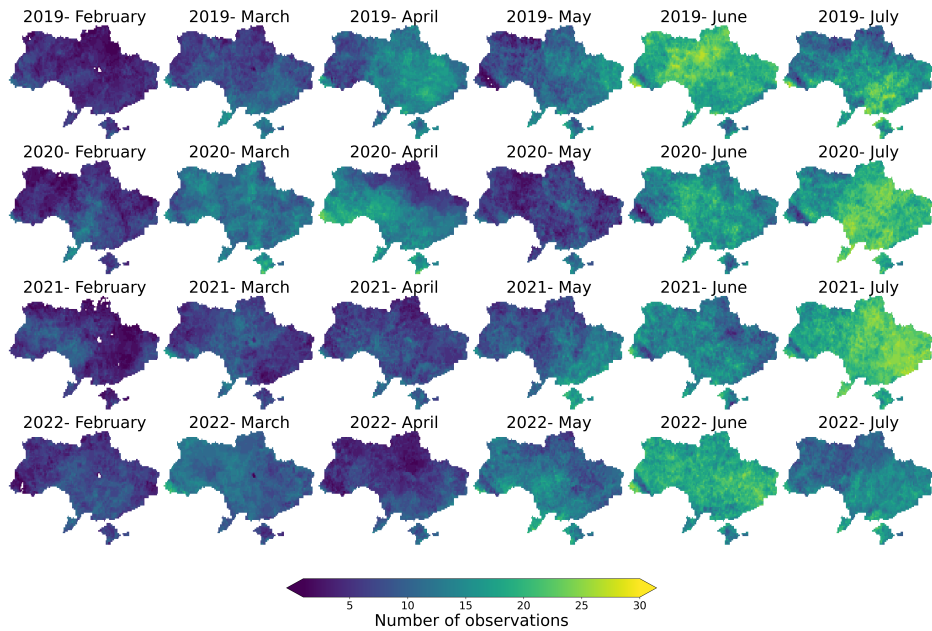


**Figure 3.4.** Monthly (from February to July) number of TROPOMI S5P NO<sub>2</sub> tropospheric columns observations for Ukraine from 2019 to 2022 using RPRO data

the time of the experiment, the RPRO data was only accessible until July 2022.

Plots presented in Figures 3.1 and 3.2 display the average monthly S5P TROPOMI NO<sub>2</sub> tropospheric column over Ukraine from 2019 to 2022 (February to July) using the ORG data and RPRO data, respectively. In 2020, a reduction of 4.8% (ORG data) and 8.3% (RPRO data) in mean NO<sub>2</sub> levels over the Ukrainian territory was observed from April to May, compared to levels recorded in 2019. In 2022, a reduction of 2.4% (ORG data) and 2.9% (RPRO data) was seen from March to July, compared to levels recorded in 2021. Additionally, during the same period, a reduction of 10.3% (ORG data) and 15% (RPRO data) was observed, compared to the NO<sub>2</sub> levels recorded in 2019. We observed that the reduction in NO<sub>2</sub> levels was more significant in the RPRO data compared to the ORG data, both during the lockdown in 2020 and the first five months (March–July) of the conflict in 2022 in Ukraine.

We summarize the number of qualified observations available for each month from 2019 to 2022 (February to July) in Ukraine using the ORG data (Figure 3.3) and RPRO data (Figure 3.4). The quantification of seasonal NO<sub>2</sub> levels can be challenging, particularly during the selected months in winter (February) and spring (March, April) of 2021 and 2022, due to the limited availability of qualified observations. This is further complicated when attempting to estimate changes before and after intervention events such as the lockdown and the armed conflict in Ukraine, as the before period falls within the winter months when observations are scarce.

### 3.2.3 Meteorological and surface NO<sub>2</sub> data

In this study, the meteorological and surface NO<sub>2</sub> data are utilized as the predictors for the estimation of NO<sub>2</sub> under BAU conditions as suggested by (Barré et al., 2021). The meteorological data is ERA5 reanalysis data which is collected from the Climate Data Store of the Copernicus Climate Change Service (Hersbach et al., 2018). We use the following weather variables: 10 m wind speed (u and v component, m/s) and direction (degrees), 2m air temperature (K), 2m dewpoint temperature (K), relative humidity (%), geopotential (m<sup>2</sup>/s<sup>2</sup>), and BLH (m). All the variables are downloaded at the original resolution of  $0.25 \times 0.25$  degree and then linearly interpolated to  $0.1 \times 0.1$  degree (about  $10\text{km} \times 10\text{km}$ ) resolution. The

utilized surface NO<sub>2</sub> data is collected from CAMS European air quality forecast and reanalyses and forecast (Marécal et al., 2015) by using the Atmosphere Data Store of the CAMS (<https://ads.atmosphere.copernicus.eu/>). Since the forecast data is a 3-year rolling archive from the present, we utilized the analysis data for 2019. The surface NO<sub>2</sub> forecast data served as the predictors under the BAU scenario for 2020 to 2022. As forecast predictions do not involve an assimilation process (Barré et al., 2021), we expect no effect of the pandemic lockdown, and the impact of the armed conflict related events on air pollution was included in the surface NO<sub>2</sub> pollution level. Both forecast and analysis data are available at the resolution of  $0.1 \times 0.1$  degree. We calculated the mean values based on data from 13:00 and 14:00 hours local time to represent the surface NO<sub>2</sub> and meteorology value at the time the satellite S5P overpassed Ukraine.

### **3.2.4 Fire spots database and Ukraine crisis hub**

In order to draw a detailed picture of the battle spots, we utilized data from Fire Information for Resource Management System (FIRMS) provided by National Aeronautics and Space Administration (NASA) and Ukraine Crisis Hub data from the Armed Conflict Location and Event Data Project (ACLED) (Raleigh et al., 2010). The NASA FIRMS portal provides active fire data at three-hour intervals based on satellite observations from products of the Moderate Resolution Imaging Spectroradiometer (MODIS) and Visible Infrared Imaging Radiometer Suite (VIIRS). For the study, data from the VIIRS product was employed to access the active fire spots due to its superior fire detection capabilities compared to the MODIS products (Csiszar et al., 2014; Schroeder et al., 2014).

Detailed data on conflict hotspot locations are extracted from the Ukraine Crisis Hub which is distributed by ACLED (Raleigh et al., 2010). Information regarding the conflict events is updated weekly and disaggregated to event type with time and location (latitude and longitude) in Ukraine and the Black Sea region available from 2018 until the present. As a result of the conflict, we expect to see and identify corresponding patterns between locations of active fire spots and the locations of conflict events.

### **3.2.5 Population data**

As NO<sub>2</sub> pollution levels are closely related to human socio-economic activities and frequently high in populous urban areas, we downloaded 2020 population data for Ukraine from the WorldPop Global Project ([www.worldpop.org](http://www.worldpop.org)), available annually at the spatial resolution of 100m×100m as one of the features for the BAU NO<sub>2</sub> model. The population data was collected, clipped to the Ukrainian territory, and linearly interpolated to 0.1×0.1 degree (about 10km×10km).

## **3.3 Business-as-usual (BAU) modelling**

When considering changes induced by the pandemic lockdown and the armed conflict, especially for before-after analysis, an important factor is the meteorology variations. In this study, we use a suggested list of predictors by (Barré et al., 2021), which consists of meteorological, spatial, and temporal features, population counts from WorldPop Global Project, and surface NO<sub>2</sub> pollution levels from CAMS European analysis data for 2019 and forecast data for 2020 to 2022 for BAU model development. The spatial and temporal features contain latitude, longitude, Julian date (number of the day from January 1), and day of the week, respectively. However, unlike the study cited (Barré et al., 2021), for machine learning model selection, instead of GBM we utilized LightGBM (Ke et al., 2017), which is a gradient boosting decision tree, to build the BAU model. During the training process, other than in studies that used the grid search with an n-fold cross-validation approach to tune the model's hyperparameters (Barré et al., 2021; Petetin et al., 2020), we employed the Fast Library for Automated Machine Learning (FLAML) (Wang et al., 2021), which is a new lightweight library for quickly determining the accurate model, to find the optimum hyperparameters for the LightGBM model in our case. In order to assess the performance of the BAU simulation model, we randomly selected and used 80% of the data for the training set and 20% for the validation set. We used the following metrics: mean bias (MB), normalized mean bias (nMB), root mean square error (RMSE), normalized root mean square error (nRMSE) and Pearson correlation coefficient (R). As shown in the detailed results presented in Table 1, the model achieved high R on the validation set (0.8 for ORG data, 0.86 for RPRO data), with low

MB and RMSE indicating that the column NO<sub>2</sub> levels are well represented by the input features. Based on the feature importance measure as shown in Figure A1, we found that the most important predictors are wind speed and direction, and BLH, which is also consistent with our hypothesis about the impact of the meteorological parameters on column NO<sub>2</sub> levels mentioned above. In Figure A2, we present the performance of the BAU model on the validation set using trend lines and scatter plots to compare the predictions with the actual ground truth data. Furthermore, Figure A3 displays the OBS data, BAU model's predictions during the lockdown period in 2020, and more than five months of the conflict (February 24–July 31) in 2022. This data is accompanied by the reference NO<sub>2</sub> levels from 2019 which were utilized to train the BAU for corresponding periods.

**Table 3.1.** The performance of the BAU model on the validation set described using the following metrics: mean bias (MB), normalized mean bias (nMB), root mean square error (RMSE), normalized root mean square error (nRMSE) and Pearson correlation coefficient (R). N represents the number of points in both the training set and validation set, where each point is associated with unique latitude and longitude values. There are no duplicate points shared between the training and validation sets.

	MB	nMB	RMSE	nRMSE	R	n
Performance with S5P data version 1.x –ORG data						
Training set	$3.68 \times 10^{-5}$	$1.53 \times 10^{-4}$	7.80	7.40	0.87	5022
Validation set	0.03	0.10	9.53	10.98	0.80	1269
Performance with S5P data version 2.4 –RPRO data						
Training set	$2.67 \times 10^{-4}$	$1.04 \times 10^{-3}$	6.97	5.12	0.91	5051
Validation set	0.07	0.26	8.47	7.75	0.86	1242

The main shortcoming of this method is the lack of qualified reference data to develop the weather normalization model under BAU conditions, as the S5P TROPOMI data has been only available since mid-2018. Only one year of training data in 2019 is considered relatively small, thus resulting in large errors in BAU simulations in winter months as during this time, limited qualified S5P observations are available and NO<sub>2</sub> pollution levels are quite unpredictable due to

City	Pre-lockdown (March 1 –15)				Lockdown (April 6 –May 10)			
	OBS-BAU		2020–2019		OBS-BAU		2020–2019	
	ORG	RPRO	ORG	RPRO	ORG	RPRO	ORG	RPRO
Kyiv	-23.7	-23.1	-30.6	-32.8	-18.8	4.9	-29.4	-21.4
Kharkiv	7.6	20.8	47.9	49.1	-0.9	-4.9	-24.1	-24.9
Odessa	5.1	29.0	4.8	22.4	6.9	21.0	-4.4	-1.9
Dnipro	1.3	1.5	17.0	16.7	-6.6	2.8	-23.9	-22.3
Donetsk	16.8	41.9	10.3	11.2	28.2	42.0	-4.0	7.2
Zaporizhzhia	11.5	1.9	0.6	-11.1	2.5	9.1	-20.1	-17.2
Lviv	32.2	35.7	-7.3	37.7	0.0	3.0	-1.2	1.4
Kryvyi Rih	-7.3	-5.3	1.2	-9.8	-6.4	0.1	-21.9	-20.5
Mykolaiv	-10.2	10.1	3.3	41.5	-0.6	13.8	-11.1	-0.4
Mean	3.7	12.5	5.2	13.9	0.5	10.2	-15.6	-11.1

the inconsistency in heating activities and NO<sub>2</sub> intake from Poland.

### 3.4 NO<sub>2</sub> changes induced by COVID-19 lockdown

The purpose of this section is to examine the effect of the lockdown on changes in NO<sub>2</sub> column levels in populous urban areas, namely the nine cities Kyiv, Kharkiv, Odessa, Dnipro, Donetsk, Zaporizhzhia, Lviv, Kryvyi Rih, and Mykolaiv (listed in declining order of population). To begin, we analyse the meteorological patterns during the pre-lockdown and lockdown periods and discuss how these might influence the NO<sub>2</sub> levels, apart from the impacts of the lockdown measures. Next, we utilize two methods to estimate changes in NO<sub>2</sub> levels. The first method, known as the year-to-year approach suggested by (Barré et al., 2021), involves calculating the median value of the actual S5P observation data in 2020 and subtracting the observation data from 2019. The second method, OBS-BAU, utilizes the median value of the actual observation data (OBS) in 2020 and subtracts the simulated NO<sub>2</sub> levels that represent the BAU scenario, which are predicted by the S5P tropospheric NO<sub>2</sub> column levels without any lockdown measures. The

BAU simulations are based on the representation of meteorological, spatial, and temporal parameters.

### **3.4.1 Lockdown and pre-lockdown meteorological patterns**

Figure 3 and Figure 4 display the probability density functions of the BLH, and wind speed and direction during the pre-lockdown and lockdown periods of 2019 and 2020 based on data from the nine selected cities. In 2020, the BLH exhibited a similar distribution to that of 2019 during the pre-lockdown period, but with lower values. This decrease in BLH would have resulted in an increase in NO<sub>2</sub> levels in 2020 compared to 2019, as the reduced BLH restricts the dispersion of NO<sub>2</sub> emissions, leading to an increase in NO<sub>2</sub> concentration levels (see Figure 3a). Conversely, during the lockdown period (see Figure 3b), we observed higher values of BLH in 2020 compared to 2019. This increase in BLH could have contributed to the dispersion of NO<sub>2</sub> concentration, resulting in a reduction of NO<sub>2</sub> levels during the lockdown in 2020. This phenomenon, in addition to the effects of the lockdown restrictions, may have also contributed to minimizing the NO<sub>2</sub> levels over major cities in Ukraine. Therefore, it is essential to consider the impacts of meteorological variables on NO<sub>2</sub> level variability analysis.

### **3.4.2 S5P NO<sub>2</sub> level changes in the most populous cities of Ukraine**

In Figures 5(a,b), and Table 2, we present the result of the year-to-year approach. We assumed that there would be a minimal change in NO<sub>2</sub> pollution levels during the pre-lockdown period, but a significant reduction during the lockdown when comparing the same time frame in 2019 and 2020 due to the implemented lockdown measures and social distancing practices. In Figure 5, two different methods, namely the OBS-BAU and year-to-year approaches, were used for the analysis. The circle size in the figures corresponds to the population of each city. For each sub-figure (a) and (b), the first row (a1, a2, b1, b2) contains two plots showing the results based on the ORG data (S5P v1.x), while the second row (a3, a4, b3, b4) includes two plots presenting the results based on the RPRO data (S5P v2.4). The left column plots (a1, a3, b1, b3) of Figures 5(a,b) display the

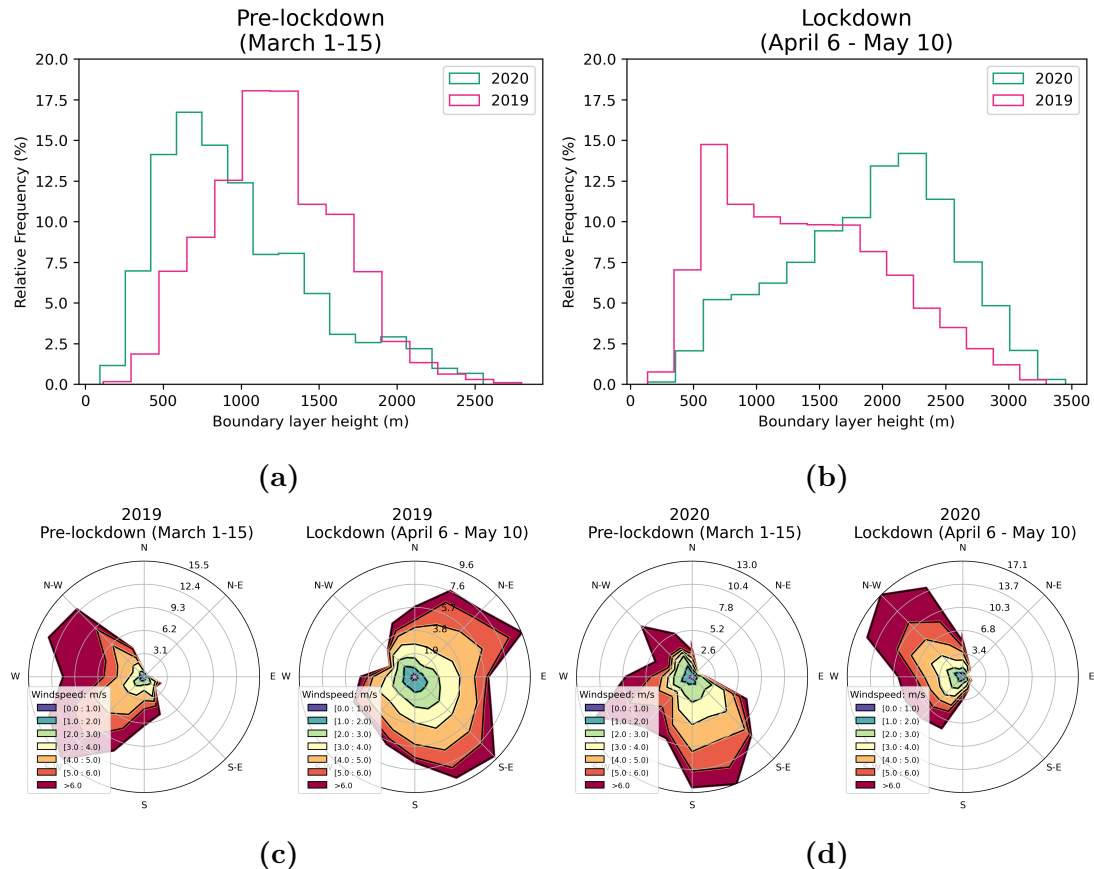


**Figure 3.5.** Probability density functions of BLH during (a) the pre-lockdown (March 1–15) and (b) the lockdown period (April 6–May 10) between 2019 and 2020 based on data from the nine most populous cities of Ukraine. Wind rose plots for wind speed and direction for pre-lockdown (March 1–15) and lockdown (April 6–May 10) periods in (c) 2019 and (d) 2020 based on data from the nine most populous cities of Ukraine

year-to-year estimates, while the right column plots (a2, a4, b2, b4) display the OBS-BAU estimates. Figure 5(a) illustrates that the prevailing trend in the nine selected cities during the pre-lockdown period showed an increase, with an average of 5.2% (ORG data) and 13.9% (RPRO data) in NO<sub>2</sub> levels, while during the lockdown period (Figure 5(b)), a general reduction was observed in most cities with an average of 15.6% (ORG data) and 11.1% (RPRO data). This confirms that the lockdown measures reduced the NO<sub>2</sub> column concentrations in major urban areas of Ukraine, as we anticipated. It is worth noting that the year-to-year approach using the original satellite observations has been widely used in many studies and online resources. However, as mentioned in (Barré et al., 2021; Grange et al., 2021), it is heavily influenced by meteorological variables such as wind speed and direction, and BLH (Wallace and Kanaroglou, 2009).

In order to quantify the true improvement in air quality with respect to column NO<sub>2</sub> levels due to the lockdown restrictions, we calculated the difference between the actual observation data and the simulated data under BAU conditions with the meteorological effects decoupled. Like the year-to-year approach, we anticipate a slight variation between the OBS NO<sub>2</sub> levels and the BAU NO<sub>2</sub> levels during the pre-lockdown period. Furthermore, we expect to observe an overall reduction in the OBS data compared to the BAU data, or at least, a lesser increase during the lockdown when compared to the pre-lockdown levels, due to the impact of the lockdown measures. Figure 5((a2, a4) and (b2, b4)) shows the OBS-BAU estimates for pre-lockdown and lockdown in 2020. During the pre-lockdown (Figure 5(a2, a4)), we observed an average increase of 3.7% (ORG data) and 12.5% (RPRO data), which is smaller than the year-to-year estimate. However, during the lockdown period (Figure 5(b2, b4)) a smaller increase trend was observed, with an average of 0.5% (ORG data) and 10.2% (RPRO data). This indicates that while the OBS NO<sub>2</sub> levels in 2020 were higher than those predicted under the BAU scenario during the lockdown period, the measures implemented during the lockdown effectively curbed the increase in NO<sub>2</sub> column concentrations in major urban areas of Ukraine when compared to the pre-lockdown levels, aligning with our initial expectations. By using the OBS-BAU estimate based on the ORG data, the most significant reduction was observed in Kyiv (18.8%), with Dnipro and Kryvyi Rih experiencing smaller reductions of 6.6% and 6.4%, respectively.

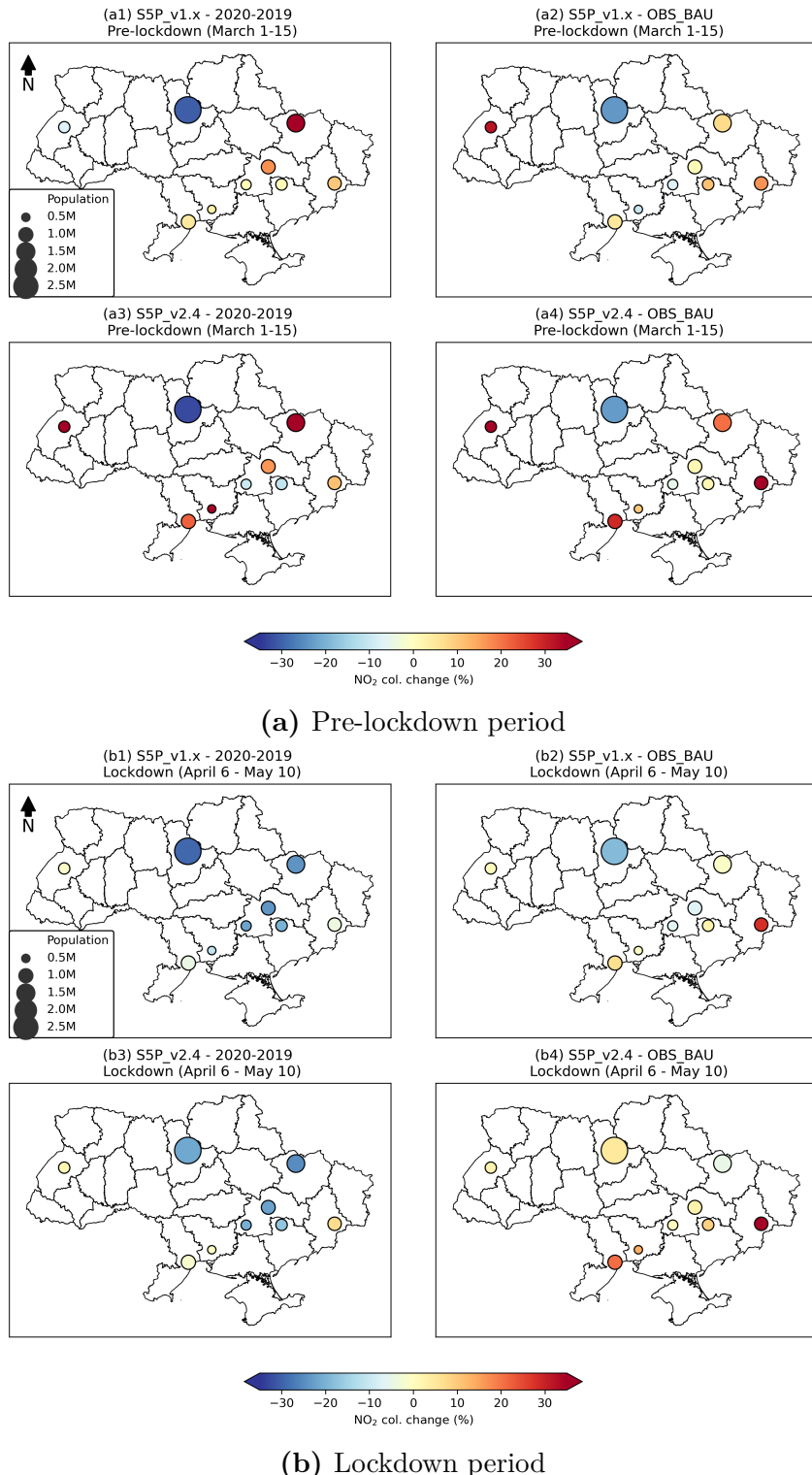


**Figure 3.6.** Estimates of S5P NO<sub>2</sub> column changes for the nine most populous cities in Ukraine during the (a) pre-lockdown and (b) lockdown periods.

However, when using RPRO data, a reduction was only seen in Kharkiv (4.9%).

In comparison with the year-to-year approach with respect to the pre-lockdown (see Table 2), the OBS-BAU estimates (3.7% for ORG data, 12.5% for RPRO data) show a smaller change than in year-to-year estimates (5.2% for ORG data, 13.9% for RPRO data). We consider the OBS-BAU estimate to be more reasonable as mentioned above, and the lower values in BLH in 2020 could result in higher year-to-year estimates during the pre-lockdown period between 2020 and 2019. Therefore, we anticipate a lower estimate, which is a smaller increase, after the weather effects are decoupled. Similar findings are seen during the lockdown for OBS-BAU and year-to-year estimates. The contribution from the lower BLH in 2019 could overestimate the reduction of NO<sub>2</sub> concentrations by 15.6% (ORG data) and 11.1% (RPRO data) in the year-to-year lockdown estimates. By normalizing the weather effects, a lower reduction in the increase is anticipated and estimated from the OBS-BAU approach (0.5% for ORG data, 10.2% for RPRO data). Additionally, the year-to-year approaches mostly present a larger standard deviation than the OBS-BAU approach, which could be attributed to local biases caused by meteorological variabilities (Barré et al., 2021). Using weather-normalization techniques, we observed that much of the reduction in NO<sub>2</sub> levels between 2020 and 2019 can be attributed to weather variability. This suggests that stricter measures may need to be considered in the future to achieve significant NO<sub>2</sub> reductions in densely populated areas of Ukraine.

### 3.5 NO<sub>2</sub> changes induced by the armed conflict

In the previous section, we discussed the influence of meteorological factors on the concentration of NO<sub>2</sub> and how using OBS-BAU estimates can mitigate overestimation or underestimation in the year-to-year approach. In this section, we shift our focus solely to the OBS-BAU estimates to explore the impacts of the armed conflict on NO<sub>2</sub> column concentration. The year-to-year estimates are displayed together for the purpose of comparison.

During the lockdown, one might reasonably assume that pollution levels were likely to decrease as the result of an anticipated reduction in socio-economic activities in major urban areas. However, trends in NO<sub>2</sub> levels during the conflict

are likely to be unpredictable in the chaos of armed conflict actions and regionally attributed to various type of emissions at multiple locations, especially at the beginning of the conflict. On one hand, the NO<sub>2</sub> levels should be expected to decline as anthropogenic emissions would be expected to decline due to minimized activities in transportation, industry and other socio-economic activities. On the other hand, surges in conflict activities – such as attacks with missiles, artillery shelling, bomb and mine explosions, etc., as well as the constant usage of military vehicles and the transportation of civilian populations from conflict zones in such a short time – could result in a rise in air pollution levels. Therefore, we extend our study beyond the most populous cities and include other territories in Ukraine affected by the conflict. To accomplish this, we begin by locating the conflict hotspots where military actions and battles took place, and then analyse the changes in NO<sub>2</sub> concentrations in the hotspots, which are highly contested zones. We estimated the changes in pollution levels from individual conflict points, and the results are presented in Section 5.1. In Section 5.2, we analyse the impacts of the conflict on NO<sub>2</sub> levels in other affected regions, such as major cities with populations exceeding 0.5 million, and the areas surrounding CPPs.

### **3.5.1 Changes of S5P NO<sub>2</sub> levels in conflict hotspot locations**

#### **Satellite-captured fire spots and statistics for conflict hotspot locations**

To understand the distribution of conflict hotspots, we utilized both the satellite-capture fire data from the NASA FIRMS portal, and in particular, the locations of battles provided by ACLED (Raleigh et al., 2010). First, we inspect the fire data from the VIIRS fire product for two consecutive years (2021 and 2022), searching for patterns representing the appearance of conflict hotspots. Then, we visually compare the pattern of fire spots captured by satellite with the reported battle locations.

Figure 6 displays the satellite-captured fire spots for 2021 (1st column), 2022 (2nd column) and locations of conflict hotspots (3rd column). We only show the similar patterns captured from the monthly NASA FIRMS product and the

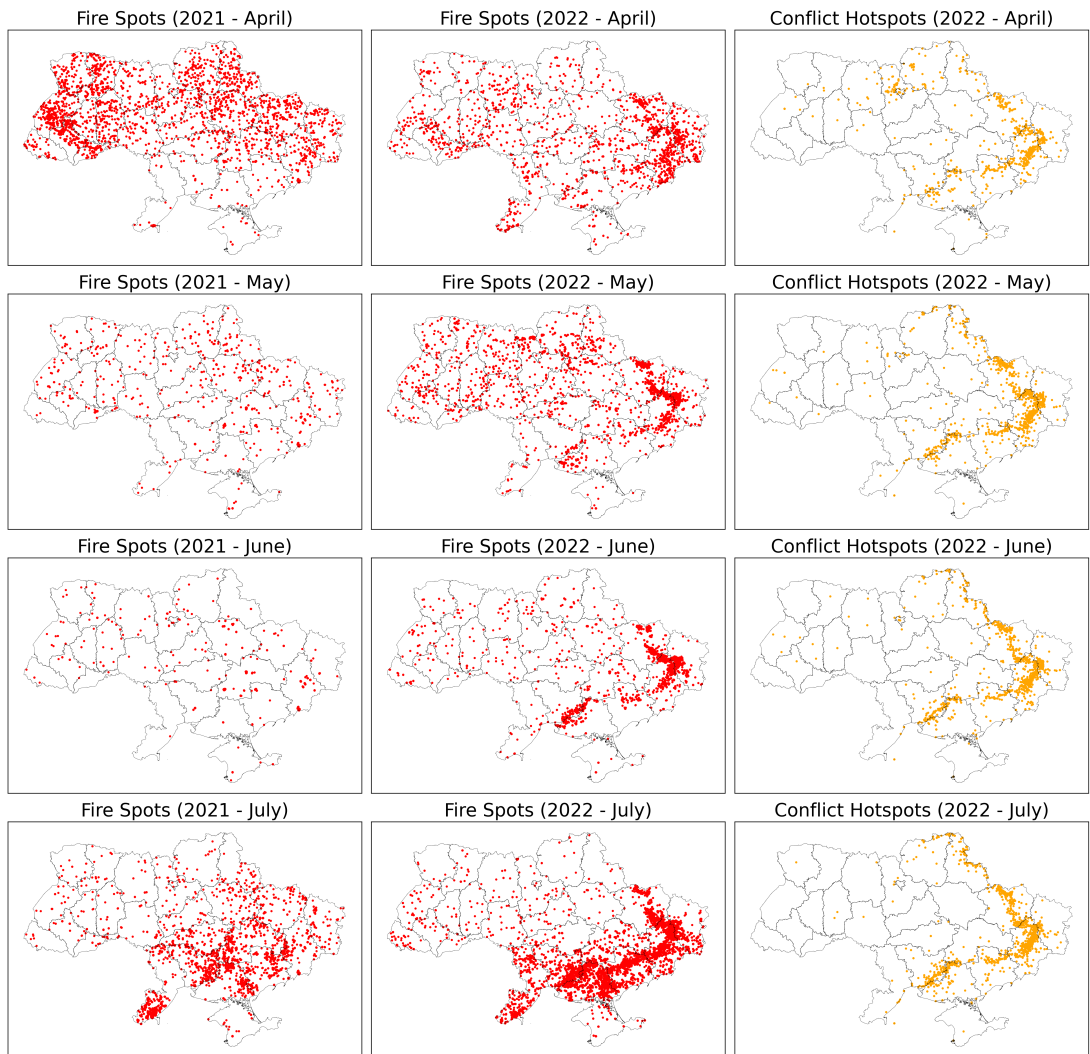


**Figure 3.7.** Satellite-captured fire spots for 2021 (1st column), 2022 (2nd column) and conflict hotspots (3rd column) in April, May, June and July. The patterns of conflict hotspots are clearly recognizable in the satellite-capture fire product from NASA FIRMS

reported conflict hotspot locations from Ukraine Crisis Hub, to avoid the overwhelming plots of 12 months. We observe that from February 24 until the end of March, the distribution of the detected fire spots forms no certain pattern and is scattered over the Ukrainian territory. From April to July 2022 the fire pattern starts to form and gradually be identifiable as similar to the conflict spots in the eastern part of the Ukrainian territory, while no special pattern is found in the 2021 figures for the corresponding periods. It is notable that the eastern region comprising of five oblasts (typically translated as regions or provinces, namely Dnipropetrovsk, Donetsk, Kharkiv, Luhansk, and Zaporizhzhia) has been at the frontline of the armed conflict and subject to intense conflict hotspots since the conflict began. Given our understanding that the ongoing armed conflict is the source of explosions and smoke, it is reasonable to assume that the conflict has resulted in a significant increase in air pollution (Pereira et al., 2022), particularly in the areas directly affected by the conflict events that are detectable via VIIRS satellite products, so we would expect that S5P observations have the capability to show the resulting impacts on both overall air quality and concentrations of NO<sub>2</sub> in the affected areas.

### Changes of S5P NO<sub>2</sub> column levels

Until March 2023, as reported by (Nichita and Ana, 2023), nearly 40,000 events related to the conflict were recorded across the Ukrainian territory by the ACLED project (Raleigh et al., 2010). The five oblasts Dnipropetrovsk, Donetsk, Kharkiv, Luhansk and Zaporizhzhia have been on the frontline of the Russia-Ukraine armed conflict since February 24, 2022. In these areas, shelling, artillery, and missile attacks accounted for 71% of conflict events recorded between February 24 and July 31, 2022 (Nichita and Ana, 2023). In order to evaluate the impacts of conflict events at the smallest level, we quantify changes in NO<sub>2</sub> column levels directly at the reported event location using OBS-BAU and year-to-year estimates for the corresponding pixel from S5P data, which is equivalent a 10 km<sup>2</sup>-area containing the event location (Figure 7).

The OBS-BAU estimates based on ORG data indicate an average increase of 0.3%, while the year-to-year estimates show a more substantial increase of 13.2%. However, when using RPRO data, we observed an 11% reduction in the OBS-

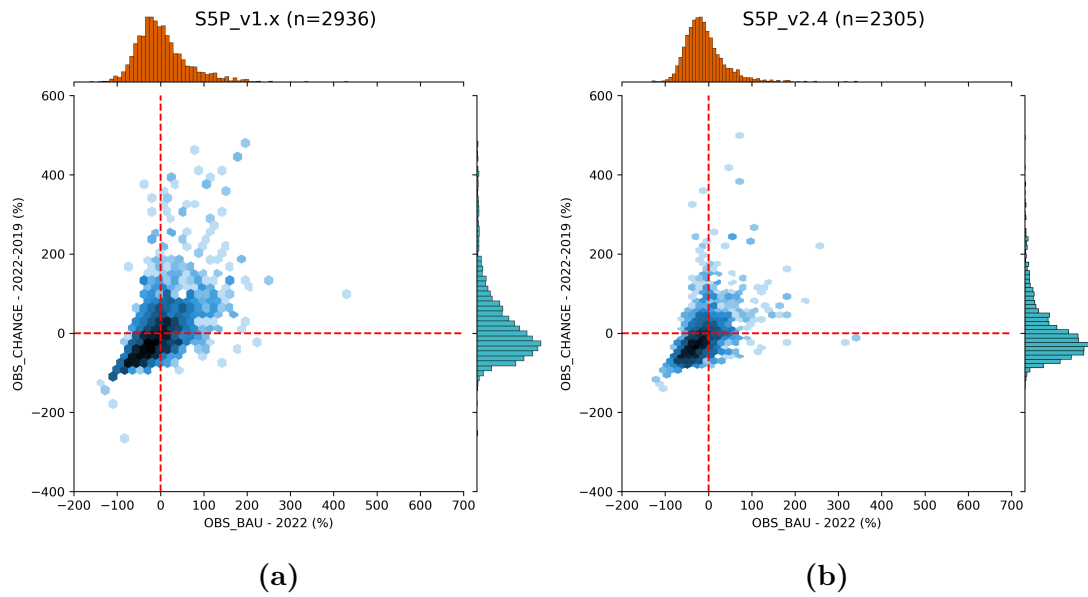


**Figure 3.8.** OBS-BAU and year-to-year estimates for the individual conflict events including air/drone strikes, armed clashes, remote explosive/landmine occurrences, shelling/artillery/missile attacks, and other forms of attacks that occurred between February 24 and July 31, 2022, for five frontline oblasts, Dnipropetrovsk, Donetsk, Kharkiv, Luhansk and Zaporizhzhia. The number of data points is denoted by (n).

BAU estimate and a 1.35% increase in the year-to-year estimate. Although there is a high level of uncertainty in estimating changes at the event location-pixel level, and the inconsistent timing between the reported conflict related events and S5P overpass may lead to an underestimation of changes in air pollution levels, the information gathered can still be useful in identifying changes in the NO<sub>2</sub> columns associated with conflict related event locations in the five oblasts.

### 3.5.2 Changes of S5P NO<sub>2</sub> levels in other affected areas

#### Most populous cities of Ukraine

In the nine most populous cities in Ukraine, both the lockdown and the conflict have led to a reduction in daily anthropogenic activities. Although this reduction was expected to lower the NO<sub>2</sub> levels, as discussed in Section 4, the lockdown measures did not result in a significant reduction in NO<sub>2</sub> column levels in 2020. To quantify the changes caused by the conflict and compare them with the effects of the lockdown measures, we analysed the OBS-BAU estimate for the most populous cities in Ukraine during the strict lockdown period from April 6 to May 10 in 2020 and 2022 (Table 3). To avoid overwhelming plots, Figure 8 displays the NO<sub>2</sub> column trend lines for OBS data and BAU predictions from February to July in 2020 and 2022 for five cities (Kyiv, Kharkiv, Dnipro, Zaporizhzhia, and Kryvyi Rih) only.

Table 3 presents the OBS-BAU estimates corresponding to the strict lockdown period (April 6 to May 10) in 2020 and 2022 for the nine most populous cities in Ukraine. Our findings indicate that the conflict has caused more significant reductions in NO<sub>2</sub> levels, compared to the lockdown measures. While minor reductions to increases were observed during the 2020 lockdown, a consistent and continuous reduction has been noticed in most cities, during the same lockdown period (April 6 to May 10) in 2022. The average reduction across all the cities of interest, as shown in Table 3, is about 12.1% (based on ORG data) and 18.1% (based on RPRO data). The largest reduction was observed in Kyiv, while the increase occurred in Lviv (14.9% based on ORG data) and in Donetsk (3.5% based on ORG data, 3.2% based on RPRO data).

In more than the first five months after the conflict began until the end of July

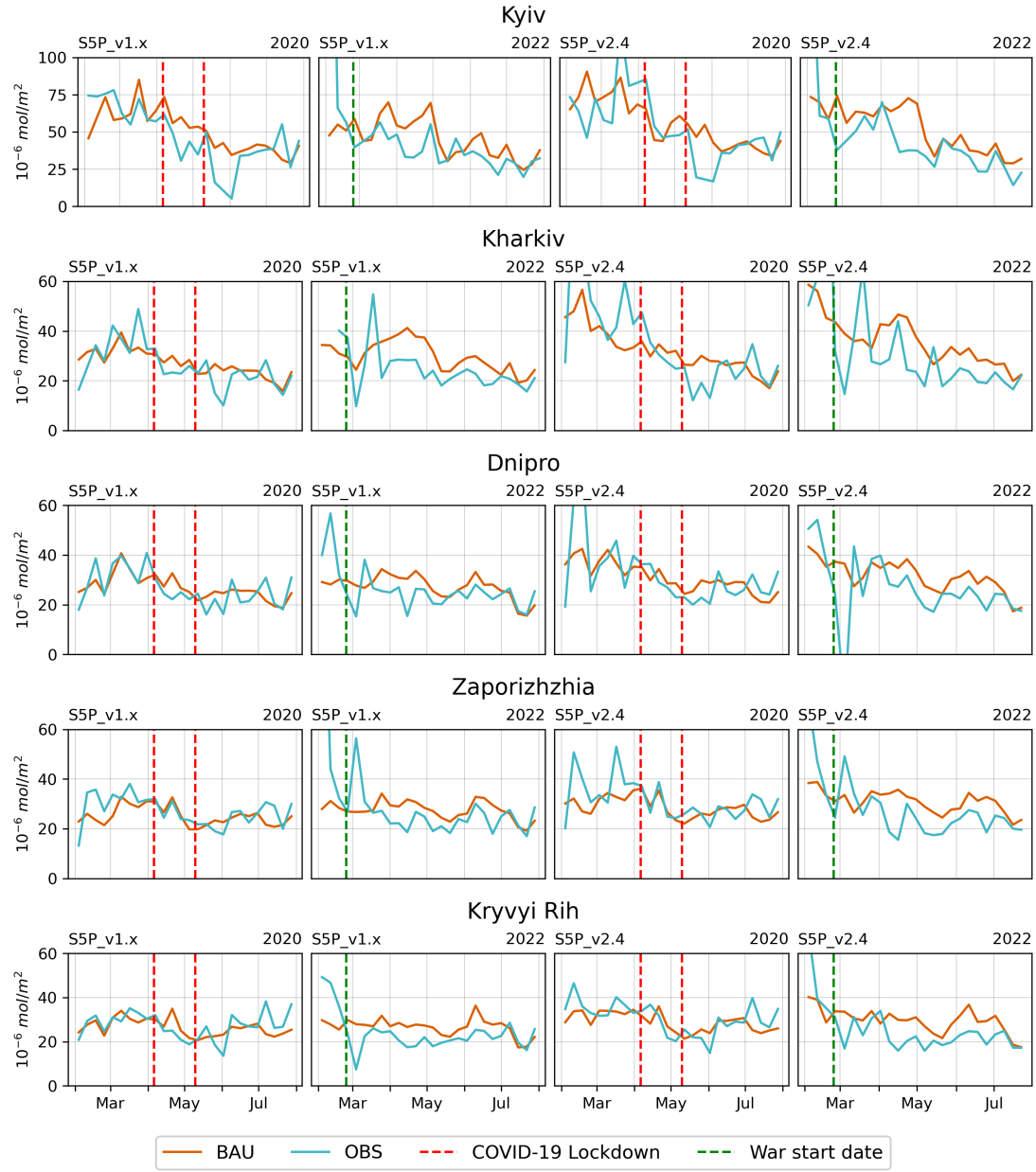


**Figure 3.9.** The trend lines of OBS and BAU S5P NO<sub>2</sub> column levels from February to July in 2020 and 2022 for five cities in Ukraine. Each row displays plots for a different city. The first and second column plots represent the ORG data (S5P version 1.x), while the third and last column plots show the RPRO data (S5P version 2.4). The first and third column plots pertain to 2020, while the second and last column plots pertain to 2022.

2022, an overall reduction is observed across the nine cities (see Table 4) with an average of 3.1% (ORG data) and 7% (RPRO data). The largest reductions in NO<sub>2</sub> levels were observed in Kyiv, with an average of 14.9% (ORG data) and 27.6% (RPRO data). Conversely, Donetsk and Lviv experienced increases in NO<sub>2</sub> levels, with both ORG and RPRO data, while in Mykolaiv only RPRO data showed the increases. The rise in Donetsk can be attributed to it being where major armed conflicts occurred during this period.

### **Coal power plants**

Besides anthropogenic activities in major cities, the contribution of CPPs to NO<sub>2</sub> concentration levels is considered to be significant in Ukraine (Lauri and Rosa, 2021). The Zaporizhzhia CPP is one of the largest emitters among CPPs in Ukraine, emitting 21,830 tonnes of NO<sub>x</sub> in 2019. Many power plants have been targeted in the conflict, and their damage or destruction has resulted in power blackouts affecting millions of people. According to Draft Ukraine Recovery Plan, Materials of the “Energy Security” Working Group covering the period to the end of June 2022, significant damage has been reported at the Zaporizhzhia, Luhansk, and Sievierodonetsk power stations, as well as other CPPs. This damage could be expected to affect NO<sub>2</sub> levels in the areas surrounding the damaged power plants. To investigate such changes, we also compare trends in the NO<sub>2</sub> column levels between OBS data and BAU simulations for 2020 and 2022, utilizing both ORG and RPRO data as presented in Figure 9. Examining an area of 10km<sup>2</sup> around each CPP, we find that, similar to previous discussions on lockdown effects, little changes are observed around most CPPs during the pandemic lockdown in 2020. However, a clear reduction is evident between the time when the conflict began and July 2022 at the Zaporizhzhia, Mironivskaya, Zmiivska, Luhansk, and Sievierodonetsk power stations. At areas surrounding other power stations, no noticeable reduction is observed.

## **3.6 Conclusion**

In this study, we performed a comprehensive assessment of variations in the S5P column NO<sub>2</sub> levels in Ukraine during the COVID-19 pandemic lockdown in

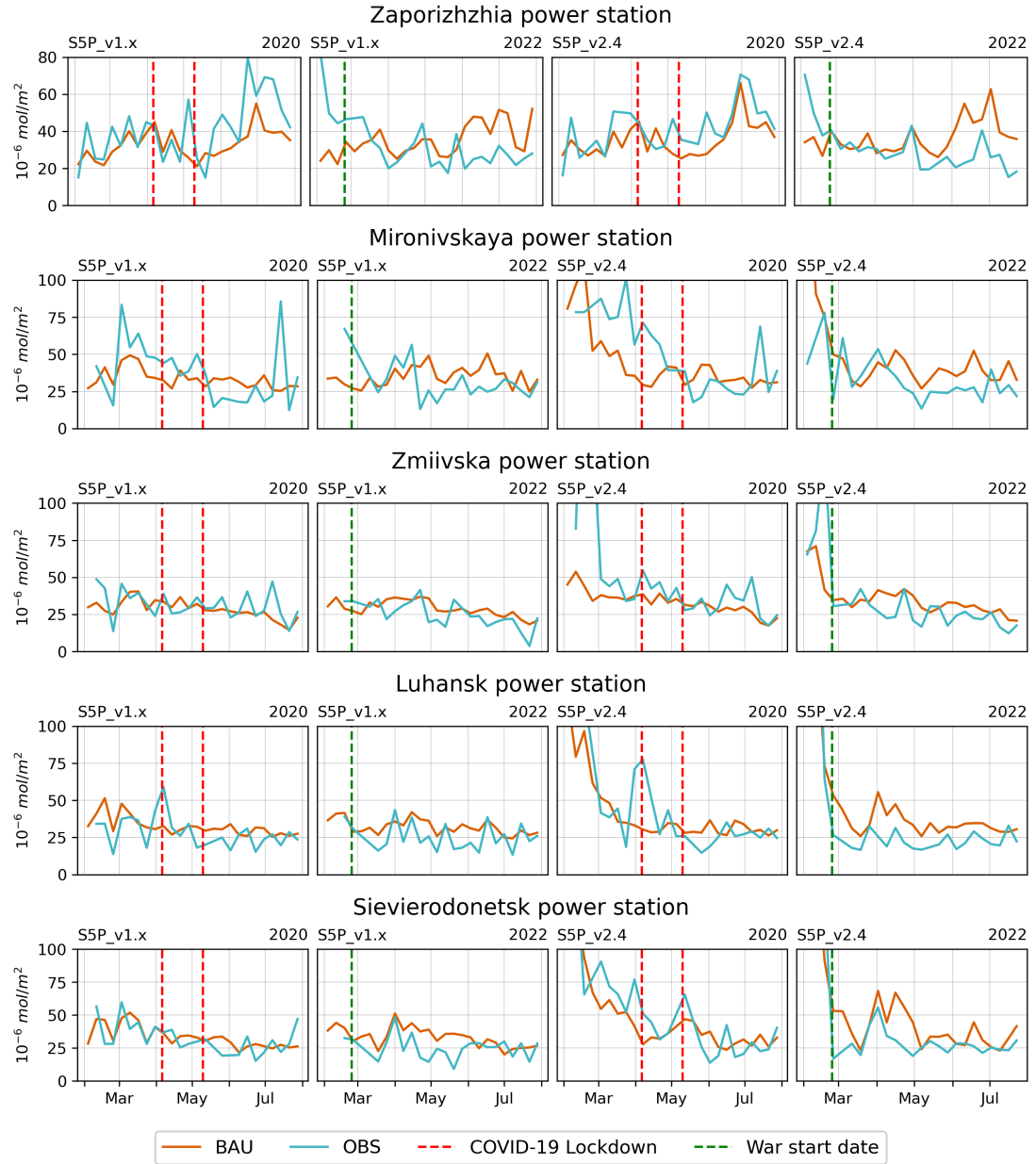


**Figure 3.10.** The trend lines for the OBS and BAU S5P NO<sub>2</sub> column levels from February to July in 2020 and 2022 are presented for selected CPPs. Each row displays plots for a different CPP. The first and second column plots represent ORG data (S5P version 1.x), while the third and last column plots show RPRO data (S5P version 2.4). The first and third column plots pertain to 2020, while the second and last column plots pertain to 2022.

2020 and the armed conflict with Russia in 2022. For this purpose, we utilized two S5P products, namely, original and reprocessing data. We first developed a weather normalization model under business-as-usual conditions, using meteorological parameters from ERA5 reanalysis, ensembled surface forecasts, and analysis NO<sub>2</sub> data from 11 CAMS models, along with other spatial and temporal features. Next, we applied the BAU prediction to estimate the change in NO<sub>2</sub> levels during the lockdown period in 2020 for the nine most populous cities in Ukraine (Kyiv, Kharkiv, Odessa, Dnipro, Donetsk, Zaporizhzhia, Lviv, Kryvyi Rih, and Mykolaiv). We extended the analysis using BAU predictions to estimate the impact of the armed conflict from February 24 to July 31, 2022, in conflict hotspot locations, the nine most populous cities, and areas surrounding selected CPPs (Zaporizhzhia, Mironivskaya, Zmiivska, Luhansk, and Sievierodonetsk) in Ukraine.

The main outcomes of the study can be summarized as follows:

- In 2020, meteorological parameters also heavily influenced the NO<sub>2</sub> tropospheric column levels, contributing to decreases in levels during the lockdown period.
- After normalizing the meteorological parameters, we found that the lockdown did not lead to lower NO<sub>2</sub> levels than the BAU prediction in 2020, although it did manage to mitigate the increase in NO<sub>2</sub> compared to the pre-lockdown period. Our study indicates that stricter measures may need to be considered in the future to achieve a significant reduction in NO<sub>2</sub> levels in densely populated areas of Ukraine.
- We observed that satellite-capture fire data from the VIIRS product can capture the spatial patterns of the conflict related events on the ground. From this product, conflict location patterns are clearly represented during the April–July 2022 period.
- Upon examining changes in NO<sub>2</sub> levels at conflict hotspots at the location-pixel level, we observed changes ranging from an 11% reduction to a slight increase of 0.3% when comparing the OBS to BAU predictions using RPRO and ORG data, respectively.

- During the strict lockdown period from April 6 to May 10, 2022, the reduction in NO<sub>2</sub> levels in the nine most populous cities was more significant compared to 2020. Across most cities, an average reduction of 12.1% (ORG data) and 18.1% (RPRO data) was observed. However, it is worth noting that Lviv and Donetsk showed an increase in NO<sub>2</sub> levels during this period.
- From February 24 to July 31, 2022, the nine most populous cities in Ukraine experienced an overall reduction of 3.1% (ORG data) and 7% (RPRO data) in NO<sub>2</sub> levels. The most significant reduction was observed in Kyiv, with an average decrease of 14.9% (ORG data) and 27.6% (RPRO data). However, in contrast, NO<sub>2</sub> levels increased in Lviv, Donetsk and Mykolaiv during this period.
- The conflict has resulted in damage to several CPPs, which are considered as major sources of NO<sub>2</sub> emissions in the country. Our analysis indicates a clear reduction in NO<sub>2</sub> levels in the areas closely surrounding Zaporizhzhia, Mironivskaya, Zmiivska, Luhansk, Sievierodonetsk CPPs.
- By utilizing the OBS-BAU estimate for both ORG data and RPRO data to analyse NO<sub>2</sub> variations during the 2022 conflict, we found that discrepancies resulting from changes in the processor during the S5P lifetime in ORG data might lead to a slight underestimation of NO<sub>2</sub> reductions. Specifically, we observed a smaller decrease using ORG data (3.1%) than with RPRO data (7%) in the most populous cities of Ukraine.

The consideration of meteorological effects is crucial in regulating pollution levels. Neglecting these effects could introduce errors in quantifying actual air quality changes attributed to an intervention event. For future studies assessing the impacts of conflict in Ukraine on air quality, it will be essential to account for meteorological variability to achieve genuine and quantitative estimates.

NO<sub>2</sub> is a significant precursor to tropospheric O<sub>3</sub> and also affects the lifetime of methane (CH<sub>4</sub>) (Akimoto and Tanimoto, 2022). Additionally, it has the potential to serve as an indicator for monitoring CO<sub>2</sub> emissions (Miyazaki and Bowman, 2023). In future studies, it would be valuable to explore how changes in NO<sub>2</sub> levels during conflict could impact O<sub>3</sub> and CH<sub>4</sub> concentrations in Ukraine as both

are important short-lived climate pollutants that contribute to positive radiative forcing, thereby exacerbating global warming.

## 4 Japan's case study

# **GREENHOUSE GAS ESTIMATION, FORECASTING AND MONITORING**

## **5 Plant functional types mapping based on scared data**

## **6 Global upscaled of carbon fluxes**

## 7 CO<sub>2</sub> monitoring and net zero modelling platform

## 8 Conclusion

  Lorem ipsum dolor sit amet, consectetur adipisicing elit, sed do eiusmod tempor incididunt ut labore et dolore magna aliqua. Ut enim ad minim veniam, quis nostrud exercitation ullamco laboris nisi ut aliquip ex ea commodo consequat. Duis aute irure dolor in reprehenderit in voluptate velit esse cillum dolore eu fugiat nulla pariatur. Excepteur sint occaecat cupidatat non proident, sunt in culpa qui officia deserunt mollit anim id est laborum.

# Acknowledgements

Thank you, and thank you.

# Bibliography

Hajime Akimoto and Hiroshi Tanimoto. Rethinking of the adverse effects of nox-control on the reduction of methane and tropospheric ozone—challenges toward a denitrified society. *Atmospheric Environment*, 277:119033, 2022.

Jérôme Barré, Hervé Petetin, Augustin Colette, Marc Guevara, Vincent-Henri Peuch, Laurence Rouil, Richard Engelen, Antje Inness, Johannes Flemming, Carlos Pérez García-Pando, et al. Estimating lockdown-induced european no<sub>2</sub> changes using satellite and surface observations and air quality models. *Atmospheric chemistry and physics*, 21(9):7373–7394, 2021.

Matthew J Cooper, Randall V Martin, Melanie S Hammer, Pieter Nel F Levelt, Pepijn Veefkind, Lok N Lamsal, Nickolay A Krotkov, Jeffrey R Brook, and Chris A McLinden. Global fine-scale changes in ambient no<sub>2</sub> during covid-19 lockdowns. *Nature*, 601(7893):380–387, 2022.

Ivan Csiszar, Wilfrid Schroeder, Louis Giglio, Evan Ellicott, Krishna P Vadrevu, Christopher O Justice, and Brad Wind. Active fires from the suomi npp visible infrared imaging radiometer suite: Product status and first evaluation results. *Journal of Geophysical Research: Atmospheres*, 119(2):803–816, 2014.

Bohdan Danylyshyn. The peculiarities of economic crisis due to covid-19 pandemic in a developing country: case of ukraine. *Problems and Perspectives in Management*, 18(2):13–22, 2020.

Carmelia Mariana Dragomir, Daniel-Eduard Constantin, Mirela Voiculescu, Lucian Puiu Georgescu, Alexis Merlaud, and Michel Van Roozendael. Modeling results of atmospheric dispersion of no<sub>2</sub> in an urban area using meti-lis and comparison with coincident mobile doas measurements. *Atmospheric Pollution Research*, 6(3):503–510, 2015.

- V. Dumitru, P. Inga, M. Danu, S. Andreas, K. Ievgen, and Y Viktoriaia. Covid-19 impact on air quality in ukraine and the republic of moldova, 2020. URL <https://www.undp.org/ukraine/publications/covid-19-impact-air-quality-ukraine-and-republic-moldova>.
- Jerome H Friedman. Greedy function approximation: a gradient boosting machine. *Annals of statistics*, pages 1189–1232, 2001.
- Noel Gorelick, Matt Hancher, Mike Dixon, Simon Ilyushchenko, David Thau, and Rebecca Moore. Google earth engine: Planetary-scale geospatial analysis for everyone. *Remote sensing of Environment*, 202:18–27, 2017.
- Stuart K Grange and David C Carslaw. Using meteorological normalisation to detect interventions in air quality time series. *Science of the Total Environment*, 653:578–588, 2019.
- Stuart K Grange, David C Carslaw, Alastair C Lewis, Eirini Boleti, and Christoph Hueglin. Random forest meteorological normalisation models for swiss pm 10 trend analysis. *Atmospheric Chemistry and Physics*, 18(9):6223–6239, 2018.
- Stuart K Grange, James D Lee, Will S Drysdale, Alastair C Lewis, Christoph Hueglin, Lukas Emmenegger, and David C Carslaw. Covid-19 lockdowns highlight a risk of increasing ozone pollution in european urban areas. *Atmospheric Chemistry and Physics*, 21(5):4169–4185, 2021.
- Hans Hersbach, Bill Bell, Paul Berrisford, Gionata Biavati, András Horányi, Joaquín Muñoz Sabater, Julien Nicolas, Carole Peubey, Raluca Radu, Iryna Rozum, et al. Era5 hourly data on single levels from 1979 to present. *Copernicus climate change service (c3s) climate data store (cds)*, 10(10.24381), 2018.
- L. Júlia, M. Dylan, R. Danielle, and B Adrian. Nearly 3 million people have left ukraine, foreshadowing a massive humanitarian crisis, 2022. URL <https://www.washingtonpost.com/world/2022/02/27/ukraine-refugees-photos-videos/>.
- Guolin Ke, Qi Meng, Thomas Finley, Taifeng Wang, Wei Chen, Weidong Ma, Qiwei Ye, and Tie-Yan Liu. Lightgbm: A highly efficient gradient boosting decision tree. *Advances in neural information processing systems*, 30, 2017.

Christine M Kendrick, Peter Koonce, and Linda A George. Diurnal and seasonal variations of no, no<sub>2</sub> and pm<sub>2.5</sub> mass as a function of traffic volumes alongside an urban arterial. *Atmospheric Environment*, 122:133–141, 2015.

M. Lauri and G. Rosa. Health impacts of coal power plant emissions in ukraine, 2021. URL <https://energyandcleanair.org/publication/health-impacts-of-coal-power-plant-emissions-in-ukraine/>.

Virginie Marécal, V-H Peuch, Camilla Andersson, Stefan Andersson, Joaquim Arteta, Matthias Beekmann, Anna Benedictow, Robert Bergström, Bertrand Bessagnet, Alberto Cansado, et al. A regional air quality forecasting system over europe: the macc-ii daily ensemble production. *Geoscientific Model Development*, 8(9):2777–2813, 2015.

Kazuyuki Miyazaki and Kevin Bowman. Predictability of fossil fuel co<sub>2</sub> from air quality emissions. *Nature communications*, 14(1):1604, 2023.

G. Nichita and M. Ana. War in ukraine one year on, nowhere safe, 2023. URL <https://acleddata.com/2023/03/01/war-in-ukraine-one-year-on-nowhere-safe/>.

Paulo Pereira, Wenwu Zhao, Lyudmyla Symochko, Miguel Inacio, Igor Bogunovic, and Damia Barcelo. The russian-ukrainian armed conflict impact will push back the sustainable development goals, 2022.

Hervé Petetin, Dene Bowdalo, Albert Soret, Marc Guevara, Oriol Jorba, Kim Serradell, and Carlos Pérez García-Pando. Meteorology-normalized impact of the covid-19 lockdown upon no<sub>2</sub> pollution in spain. *Atmospheric Chemistry and Physics*, 20(18):11119–11141, 2020.

Clionadh Raleigh, rew Linke, Håvard Hegre, and Joakim Karlsen. Introducing acled: An armed conflict location and event dataset. *Journal of peace research*, 47(5):651–660, 2010.

Mykhailo Savenets. Air pollution in ukraine: a view from the sentinel-5p satellite. *JOURNAL OF THE HUNGARIAN METEOROLOGICAL SERVICE*, 125(2):271–290, 2021.

Quirin Schiermeier. Why pollution is falling in some cities—but not others. *Nature*, 580(7803):313, 2020.

Wilfrid Schroeder, Patricia Oliva, Louis Giglio, and Ivan A Csiszar. The new viirs 375 m active fire detection data product: Algorithm description and initial assessment. *Remote Sensing of Environment*, 143:85–96, 2014.

Andrii Shelestov, Hanna Yailymova, Bohdan Yailymov, and Natalia Kussul. Air quality estimation in ukraine using sdg 11.6. 2 indicator assessment. *Remote Sensing*, 13(23):4769, 2021.

Zongbo Shi, Congbo Song, Bowen Liu, Gongda Lu, Jingsha Xu, Tuan Van Vu, Robert JR Elliott, Weijun Li, William J Bloss, and Roy M Harrison. Abrupt but smaller than expected changes in surface air quality attributable to covid-19 lockdowns. *Science advances*, 7(3):eabd6696, 2021.

T.F. Stocker, G.-K. Plattner D. Qin, M. Tignor, S.K. Allen, J. Boschung, A. Nauels, Y. Xia, V. Bex, and P.M. Midgley. Ipcc, 2013: Climate change 2013: The physical science basis. contribution of working group i to the fifth assessment report of the intergovernmental panel on climate changes. Technical report, Cambridge University Press, Cambridge, United Kingdom and New York, NY, USA, 2013.

Jos Van Geffen, Henk Eskes, Steven Compernolle, Gaia Pinardi, Tijl Verhoelst, Jean-Christopher Lambert, Maarten Sneep, Mark Ter Linden, Antje Ludewig, K Folkert Boersma, et al. Sentinel-5p tropomi no 2 retrieval: impact of version v2. 2 improvements and comparisons with omi and ground-based data. *Atmospheric Measurement Techniques*, 15(7):2037–2060, 2022.

Julie Wallace and Pavlos Kanaroglou. The effect of temperature inversions on ground-level nitrogen dioxide (no2) and fine particulate matter (pm2. 5) using temperature profiles from the atmospheric infrared sounder (airs). *Science of the Total Environment*, 407(18):5085–5095, 2009.

Chi Wang, Qingyun Wu, Markus Weimer, and Erkang Zhu. Flaml: A fast and lightweight automl library. *Proceedings of Machine Learning and Systems*, 3: 434–447, 2021.

Rasa Zalakeviciute, Danilo Mejia, Hermel Alvarez, Xavier Bermeo, Santiago Bonilla-Bedoya, Yves Rybarczyk, and Brian Lamb. War impact on air quality in ukraine. *Sustainability*, 14(21):13832, 2022.